

# SPATIO-TEMPORAL CHANGES OF CHLOROPHYLL CONCENTRATION WITH ENVIRONMENTAL PARAMETERS OVER THE GULF OF MANNER, INDIA

Tholkapiyan. M<sup>\*†</sup>, Veeramalai Sankaradass<sup>\*\*</sup>, Hariharasudhan. C<sup>\*</sup>, Priyanka. M<sup>\*3</sup>, Kalaivani Ravisundar<sup>\*\*\*</sup>

\*Department of Civil Engineering, Chennai Institute of Technology, Chennai, Tamil Nadu, India.

\*\*Dept. of Computer Science and Engineering, Chennai Institute of Technology, Chennai, Tamil Nadu, India.

\*\*\*Department of ECE, Saveetha Engineering college, Chennai, Tamil Nadu, India.

†Corresponding Author: Tholkapiyan.M; [m.tholkapiyan@gmail.com](mailto:m.tholkapiyan@gmail.com)

ORCID iD: 0000-0003-1948-663X

## Abstract:

The present study investigated about the spatio-temporal analysis of chlorophyll concentration with the variation of environmental parameters such as Aerosol optical depth (AOD) and sea surface temperature (SST) over the Gulf of Mannar (GOM) located in the southeastern part of India. The data derived from several satellites were already provide information about the aquatic environment throughout the global waters. This study utilized the standard algorithms for the retrieval of Chl-a from the Moderate resolution Imaging Spectroradiometer (MODIS) satellite sensor for a time period of about 2002-2020. The monthly spatio-temporal variability of the Chl-a concentration with the changes in SST and AOD were analysed over the Gulf of Mannar for the year of 2011 has been investigated. This shows that many areas in Gulf of Mannar has high chlorophyll concentration of about 2 to 5 mg m<sup>-3</sup> in the single day images for several months during 2011. Also, the variation in the SST is observed for several months during 2011 which ranges from 28 to 31.5°C. The AOD values fall in the range of 0.09 to 0.12. In addition, the time series analysis of *Chl*, *SST* and *AOD* were also studied for two different stations over the GOM. The result of the time series analysis explains that high chlorophyll concentration was observed during the colder months with low values in *SST* and *AOD*.

Key Words	Ocean, chlorophyll, Sea Surface Temperature, Water Quality, Aerosol Optical Depth
DOI	<a href="https://doi.org/10.46488/NEPT.2025.v24i03.D4257">https://doi.org/10.46488/NEPT.2025.v24i03.D4257</a> (DOI will be active only after the final publication of the paper)
Citation of the Paper	Tholkapiyan. M, Veeramalai Sankaradass, Hariharasudhan. C, Priyanka. M, Kalaivani Ravisundar, 2025. Spatio-temporal changes of chlorophyll concentration with environmental parameters over the Gulf of Manner, India. <i>Nature Environment and Pollution Technology</i> , 24(3), B4257. <a href="https://doi.org/10.46488/NEPT.2025.v24i03.B4257">https://doi.org/10.46488/NEPT.2025.v24i03.B4257</a>

## 1. Introduction:

Chlorophyll-a (*Chla*) is the important water quality index in both marine and coastal environment. Chl-a in the ocean is the indicator of phytoplankton biomass (Gitelson et al., 1993) and primary productivity (Cannizzaro and Carder, 2006, Huot et al., 2007). Phytoplankton are microscopic plants that form the base of the marine food web, and their growth and distribution are influenced by various environmental factors. Chl-a is the most abundant pigment in phytoplankton (Patissier et al., 2014). *Chl*-a is the biological component accessible to remote sensing (via ocean color) and provides a key metric for assessing the health

and productivity of marine ecosystems on global (Gurlin et al., 2011). *Chl-a* absorbs sunlight, carbon dioxide from the earth and maintains the primary production (Hu et al., 2012), which is good for overall ocean health. It is responsible for the appearance of green pigments in plants and algae (Platt and Sathyendranath, 2008). When the chlorophyll concentration increases, the colour of the water slightly varies from blue to green. This indicates the increase in phytoplankton population (Simon and Shanmugam, 2012). Regular monitoring is necessary for assessing the blooms and implementing efficient management strategies, to avoid the deterioration of water quality (Le et al., 2013).

The extension of three different one-dimensional OCDMA codes into three-dimension OCDMA system for improved performance. The three distinct codes are the non-mapping, MS, and MD. The extensions are such that spectral domain utilises the non-mapping code, time spreading uses the MS code, and spatial domains extend with MD code (Veeramalai Sankaradass et al., 2024).

The growth of phytoplankton is often limited by the availability of nutrients such as nitrogen, phosphorus, and silica. Areas with upwelling or high nutrient input typically have higher chlorophyll concentrations. The increase in nutrient supply primarily increases the phytoplankton growth rate (Banse et al., 1996). The chl-a concentration is mainly affected by the environmental and climatic factors such as rainfall, currents, seasonal atmospheric cycles, inland river water inflow, local wind regimes, water column stratification and sea surface temperature (SST) volatilities (Tian et al., 2016).

Sea Surface Temperature (SST) is the important parameter that affects the phytoplankton growth rates and community composition. Extreme temperatures can inhibit phytoplankton growth or lead to harmful algal blooms. Variation in SST can affect the marine ecosystem in various ways (Brochier et al., 2013). According to Intergovernmental Panel on Climate Change (IPCC), global sea surface temperature is expected to rise by approximately 0.4 to 1.1°C by 2025. Change in surface temperature affects the plant and animal species present in the ocean. Increase in SST may decrease the Chl-a concentration and affect the circulation pattern that brings nutrients from the deep sea to surface water. An excessive increase in SST destroys the growth of phytoplankton and another factor that affect the growth is the amount of nutrients loaded with freshwater from river discharge (Nurdin et al., 2013). Changes in sea surface temperature and chl-a concentration may lead to global warming (Gunasinghe et al., 2024, Mondal and Lee, 2024).

The Chl-a concentration can also get affected, when change in salinity occurs due to evaporation of seawater (Al-Tae, 2018). When the wind speed increases, the evaporation rate also increases, that cause the change in salinity and chl-a concentration (Mahpeykar and Khalilabadi, 2021). Aerosols are rich source of nutrients that increase the production of marine environment and their carbon sequence (Paytan et al., 2009). Aerosols contain a variety of natural and synthetic compounds, including mineral dust, sea salt crystals, bacteria, and other microscopic particles. Aerosols are solid or liquid particles suspended in the atmosphere, with a diameter of approximately 0.001 to 100  $\mu\text{m}$  (Giles et al., 2019). Aerosol particles not only affect the radiative forcing of the Earth's air system but also influence climate and cause environmental problems such as acid rain and haze (Li et al., 2018; Huang and Ding, 2021). High concentrations of aerosols cause serious threat to human health (Morozova and Mironova, 2015). The properties of aerosols include parameters such as aerosol optical depth

(AOD), single-scattering albedo, scattering phase function, and absorbing optical depth. AOD is the most important parameter which is defined as the integral of the aerosol extinction coefficient in the vertical direction. This describes the attenuation effect of aerosols on light and is an important indicator of the level of air pollution.

Estimating Chl-a concentration using the remote sensing data is challenging in turbid and productive waters. It is difficult to monitor the changes in the *Chl-a* concentrations through field measurement and cost high. This can be overcome by using the satellite measurements through remote sensing technique, which is of low cost with high efficiency. Several studies have been conducted to monitor the water quality in large scale using the remote sensors (Le et al., 2013, Tong et al., 2022, Koponen et al., 2007). Satellite sensors provide reliable global ocean coverage of Chl-a and SST at relatively high spatial and temporal resolution. The spatial and temporal distribution can be effectively measured from the space (Ishizaka, 2010).

Several satellites like Coastal Zone Color Scanner (CZCS), Sea-viewing Wide Field-of-View sensor (SeaWiFS), Moderate Resolution Imaging Spectrometer (MODIS), Medium Resolution Imaging Spectrometer (MERIS) and VIIRS, etc. are used to derive Chl-a products from the ocean and coastal waters. NASA CZCS launched in 1978, is designed to monitor ocean color. Ocean and Land Color Instrument (OLCI) onboard the sentinel-3 satellite is introduced to monitor water quality in turbid lakes. OLCI satellite includes 21 spectral bands, improved signal-to-noise ratio (SNR), cameras for mitigation of sun glint, a global spatial resolution of 300 m, daily revisit times, and enhanced coverage. Several research have been attempted to map Chl-a concentration based on OLCI images in various turbid lakes (Pahlevan et al., 2020, Shen et al., 2020).

Satellite remote sensing is the best way to view the entire ocean surface and to monitor Chl-a at high spatial and temporal resolution (Brewin et al., 2021). To derive Chl-a, remote sensing has employed empirical algorithm (Dierssen, 2010) and semi-analytical algorithms (IOCCG, 2006). Empirical algorithm known as ocean color algorithm, use absorption properties of Chl-a and remote sensing reflectance to eliminate Chl-a from the space (O'Reilly and Werdell, 2019, O'Reilly et al., 1998). Semi-empirical algorithm uses physical models of light interactions with water to eliminate the Chl-a (Werdell et al., 2018).

Remote sensing reflectance ( $R_{rs}$ ) is determined from the inherent optical properties (IOPs) of water and optically active water constituents (OAC) (Gorden et al., 1988, Mobley, 1999). Estimation of Chl-a from  $R_{rs}$  can be analytically approached by forward or inverse modelling or by empirically associated variability of  $R_{rs}$  with one or more wavebands (Schalles, 2006). When the phytoplankton increases in ocean, the shift of reflectance is observed from blue to green wavelengths caused by the combination of increased absorption and particulate backscattering process (Morel and Prieur, 1977). This observation is then converted as most widely used Ocean Color (OC) algorithm, in which several variations occur for specific sensors (O'Reilly et al., 1998, O'Reilly and Werdell, 2019). The empirical algorithms are specially designed to estimate Chl-a from waters with high algal biomass and identifying algal blooms based on peak height methods (Matthews et al., 2012).

Several studies have been conducted for understanding the variability of Chl-a in coastal waters using the satellite sensors. Chen et al., 2013 presents Chl-a concentration retrieval in the coastal waters of Bohai, Yellow and East China sea. The in-situ data were collected and are

used to assess the performance of HY-1C in retrieving the Chl-a. The result of this study shows that the algorithm based on blue-green band ratios performed well and the broadband channel of HY-1C CZ1 can retrieve Chl-a in turbid waters. Alexander et al., 2010 made a comprehensive study on algorithm in retrieving the Chl-a from the coastal waters. The two and three band algorithms are tested with the bands that matched the spectral channels of MERIS.

In this study, the changes in *Chl-a* concentrations are analysed with SST and AOT using the MODIS satellite images. The study is conducted in the Gulf of Mannar, where the coastal waters are dominated with Chlorophyll-a are monitored using the satellite sensors. Here, the OC3 algorithm is used for the retrieval of Chl-a from Rrs. The analysis includes the spatio-temporal analysis of *Chl-a* with AOT and SST variation using the monthly images over the year of 2011. Further the study extended to the time series analysis of Chl-a with the changes of environmental parameters such as AOD and SST were analysed over the year of 2000-2020.

## **2. Study Area:**

Gulf of Mannar (GOM) (8.47°N 79.02°) located in Indian ocean between the Southeastern India and Western Sri Lanka. GOM extends from Tuticorin to Rameswaram Island in the SE-NE direction. There are 21 islands situated at an average distance of about 8 km from the coast and running almost parallel to the coastal line. GOM has a rich and diverse fauna compared to other regions. GOM region is enriched with several habitats like Coral reef, mangroves, sea grasses, sea weeds etc. GOM is the biological rich area and identified with more than 4223 species of flora and fauna. Gulf of Mannar has always moderate to the high level of chlorophyll-a present in the nearshore waters along the Indian coast.

The stations used for the analysis are shown in fig 1. The study area of station 1 with a latitude of 9.7138 and longitude of 79.1568 is located near the coastal region which is shallow water and the station 2 with a latitude of 9.3199 and longitude of 79.2026 is located near to the Pamban bridge. In Gulf of Mannar, the water temperature is influenced by the atmospheric temperature. From January to April, the temperature steadily increases with a highest peak of 32° C in May. And till august, the temperature gradually decreases. Between September and October, the temperature again increases and falls between December and January. The water temperature may exceed the atmospheric temperature during summer, in shallow region closer to land.

In Gulf of Mannar, the Chl-a concentration is high during the northeast monsoon. Because, the cold water has high Chl-a than the warm water, that contains nutrients comes from the deep ocean (Balasubramanian and Shanmugam, 2015). SST are mostly cooler than the nearby waters where the ocean current cause upwelling and the Chl-a concentration is high. Gulf of Mannar, being a tropical region has warm climate with low change in surface temperature (Tholkapiyan, 2012). It is easier for the deep water to rise to the surface, when the surface water is cold.

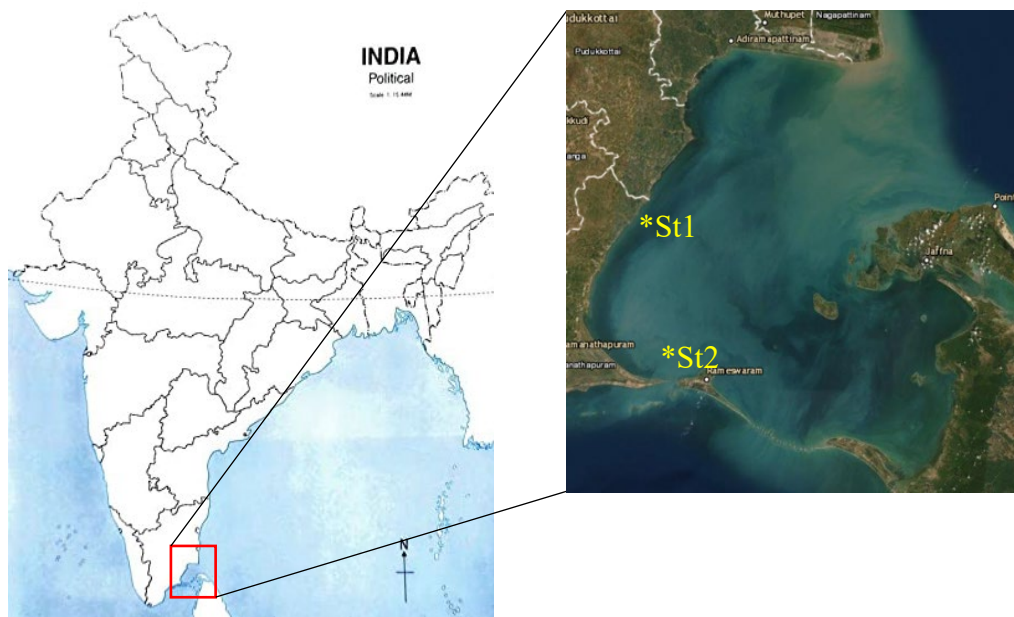


Fig.1 The location of the study area over the Gulf of Mannar in the south-east coastal waters of India (Left side). The data from stations st-1 and st-2 are used for the time series analysis (right side).

MODIS Aqua satellite data is used for accurately mapping the Chl-a concentration in the coastal water of Gulf of Mannar. MODIS is a satellite-based sensor used to measure the climatic conditions. Terra (EOS AM, launched in 1999) and Aqua (EOS PM, launched in 2000) satellite are the two MODIS sensor. MODIS sensor can capture data in 36 spectral bands ranging wavelength from  $0.4 \mu\text{m}$  to  $14.4 \mu\text{m}$  and at varying spatial resolutions. The captured data from the top of atmosphere provides  $R_{rs}$  after undergoing atmospheric correction. These  $R_{rs}$  dataset is used to monitor the measurements in large scale global dynamics including earths cloud cover, process occurring in the ocean, land and in lower atmosphere. MODIS sensor plays a major role in predicting the global changes accurately.

Using the MODIS Aqua sensor, the daily images for the two stations of Gulf of Mannar are collected over the year 2000 to 2020 from the Ocean color website. The collected data is then processed, and atmospheric correction is carried using the ACOLITE software (Pahlevan et al., 2021). The ACOLITE processor was used to correct the atmospheric effects using the dark spectrum fitting (DSF) (proposed by Vanhellemont and Ruddick, 2018 and Vanhellemont, 2019) over SWIR-based exponential extrapolation. Sun glint effect can also be removed using the ACOLITE processor. Using the satellite images, the Chl-a is estimated with good spatial resolutions.

### 3. Materials & Methods:

In this study, *Chl-a* concentration was analysed with *SST* and *AOD* using the Moderate resolution imaging spectroradiometer (MODIS) satellite sensor for 20years from 2000-2020. The standard atmospheric correction procedure (Bailey et al., 2009) is used to perform the atmospheric correction process in which the top-of-atmosphere radiance received by sensors is converted to surface reflectance. OC3 Chlorophyll algorithm is used to retrieve the *Chl-a* from the remote sensing reflectance ( $R_{rs}$ ), which is developed based on the semi analytical and bio-

optical remote sensing reflectance,  $R_{rs}$ . The sea surface temperature (*SST*) measurement and Aerosol optical depth (*AOD*) is also derived for this analysis from the MODIS satellite sensor. The variation in the chlorophyll concentration, Aerosol optical depth measurement and surface temperature analysis is presented in this study.

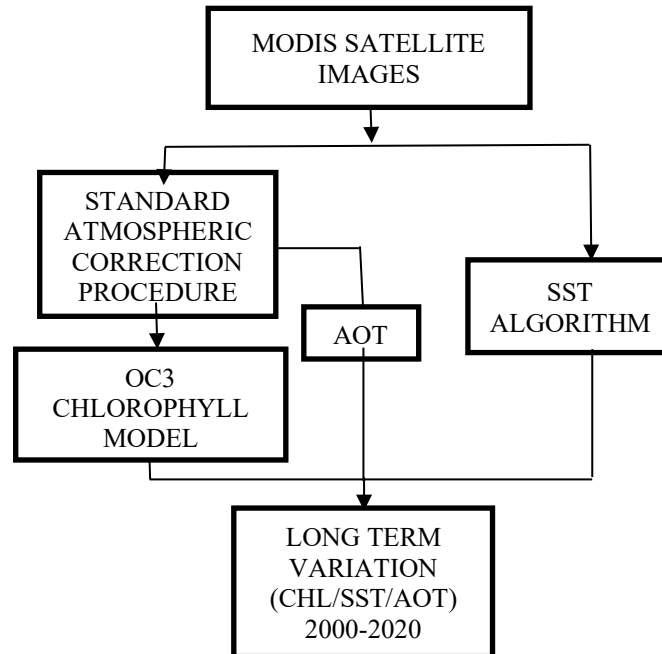


**Fig.2:** The schematic block diagram represents the methodology for the estimation of Chl-a concentration, AOT and SST for understanding their long-term changes by processing the MODIS satellite sensor data from 2000-2020.

Atmospheric correction is a crucial step in remote sensing for accurately estimating surface properties like chlorophyll-a (Chl-a) concentrations from satellite data (Gordon and Wang, 1994). The aim of atmospheric correction is to remove or correct the effects of the atmosphere on the observed radiance, which includes scattering and absorption of light by atmospheric particles and gases. Atmospheric correction algorithm is the estimation of spectral aerosol reflectance  $\rho_a(\lambda)$ , subtracted from total measured signals  $R_{rs}(\lambda)$ . NASA Ocean Biology Processing Group (OBPG) implemented an algorithm that (Gordon and Wang 1994) requires an assumption of negligible water-leaving reflectance in the NIR of the spectrum (i.e.,  $R_{rs}(\text{NIR}) = 0 \text{ sr}^{-1}$ ).

Ocean Color remote sensing involves, estimation of concentration in ocean by measuring the variation in spectral quality of the water surface. OC is obtained from the incident light interactions with other substances present in water (Chl-a concentration, suspended sediments and CDOM). These substances are quantified by water leaving radiance which is measured in the visible portion of electromagnetic radiation. OC algorithm is band-ratio based algorithm used for the retrieval of Chl-a from the remote sensing reflectance,  $R_{rs}$ . In empirical OC algorithm, Chl-a has log normal distribution which means, the model is trained on log transformed (with base 10) in situ measured Chl-a. OC3 algorithm uses quadratic polynomial with single explanatory variable. For OC3 algorithm, the numerator is the maximum of the

bands Rrs 443 and Rrs 488 and the denominator with Rrs 551. The OC3 algorithm uses a three-band blue-green reflectance ratio is defined as

$$R = \log_{10} \left[ \frac{Rrs443 > Rrs488}{Rrs551} \right] \quad (1)$$

$$Chl-a = 10^{0.28 - 2.753R + 1.457R^2 + 0.659R^4}$$

where, *Chl-a* is Chlorophyll-a concentration mg·m<sup>-3</sup>, *R* is Blue-green band ratio. OC-3 algorithm has been used to retrieve low as well as high *Chl-a* concentration and also useful in monitoring the waters from estuarine regions using spatial resolution sensors (Morel and Maritorena, 2001).

SST maps are based on observations by the MODIS Aqua satellite. The temperature estimated from the satellite measurements are known as brightness temperatures (BT). SST measured at the sea surface is not same as the satellite derived SST because of atmospheric interference. So, for the identification or removal of clouds and aerosols contribution in satellite radiance, atmospheric correction procedure was followed. The bands which provide more information for the correction procedure are the atmospheric windows at the wavelength range of  $\lambda = 3.5\text{--}4.1 \mu\text{m}$  and  $\lambda = 9.5\text{--}12.5 \mu\text{m}$  (McMillin, 1975). Although the two spectral channels provide BT, but the magnitudes of the retrievals are different based on the atmospheric transmissivity. The difference in brightness temperature is defined as the temperature drop of SST and other BT (McMillin, 1975 and Barton, 1995), which provides the linearized relation in terms of multi-channel sea surface temperature equation. The equation is as follows:

$$SST = aT_i + \gamma(T_i - T_j) + c \quad (2)$$

where  $\gamma$  is the coefficient of differential absorption,  $T_i$  and  $T_j$  are the brightness temperature obtained from the two channels. MODIS Aqua/Terra, have two bands in the transmission window. The robust algorithm as follows:

$$SST = a_0 + a_1T_{3.95} + a_2(T_{3.95} - T_{4.05}) + a_3(\sec(\theta) - 1) \quad (3)$$

Here, the coefficients of the equation such as  $a_0$ ,  $a_1$ ,  $a_2$ , and  $a_3$  are obtained from Kilpatrick et al., 2015. The above method has been applied to produces satellite-derived SST for the temporal and spatial analysis and the SST retrieval from the MODIS images.

#### 4. Results and Discussion:

This section describes the results in two subsections: one is the spatio-temporal analysis and second one is time series analysis. The spatio-temporal analysis of *Chl-a* concentration, AOD and SST are presented for one year (2011) with the monthly images. The time series analysis is carried out to investigate the possibility of a significant trend in the *Chl*, SST and AOD over the span of 19 years.

##### 4.1. Spatio temporal analysis

The above figures represent the *Chl-a*, *AOT* and the *SST* measurements over the Gulf of Mannar by MODIS satellite sensor for the 6-month duration from January to June 2011. The variability of *Chl-a* concentration with the changes in *SST* and *AOT* over the Gulf of Mannar is presented in this study. Fig.3a. represents the *Chl-a* concentration and the color bar represents the relative changes corresponding to dimensional trend with respect to *Chl-a* concentration.

Fig.3b represents the Aerosol optical depth measurement and the color bar indicates the relative change with respect to the aerosol measurement. And the fig.3c represents the surface temperature and the color bar indicates the relative changes with respect to sea surface temperature.

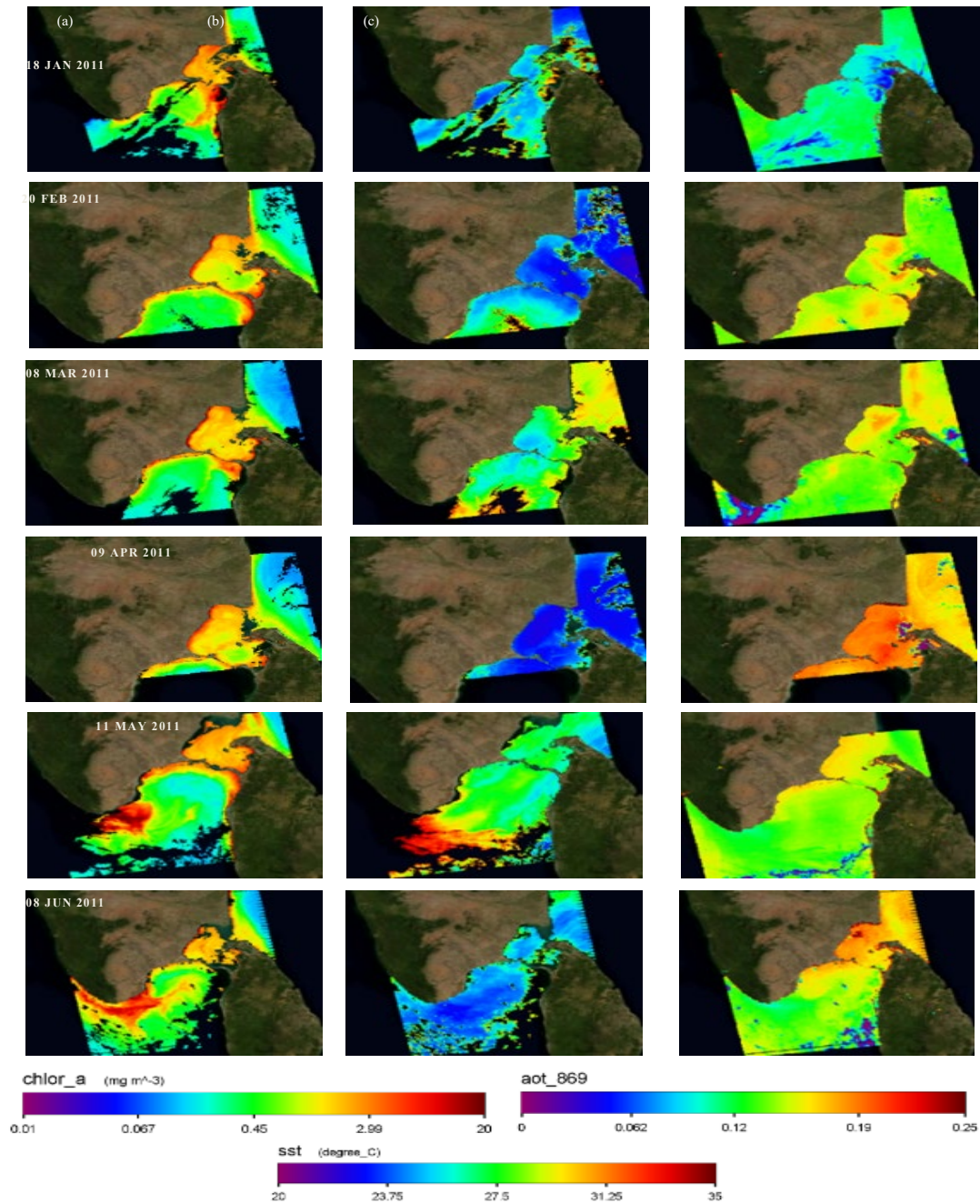


Fig.3. (a) Chl-a concentration trend over Gulf of Mannar by using MODIS satellite sensor for the duration of 6-month from January to June 2011, (b) Aerosol optical depth and (c) Sea surface temperature measurement during the study period. Color bar scale represents the relative changes corresponding to the dimensional trend with respect to the Chl-a concentration, AOT and SST values.

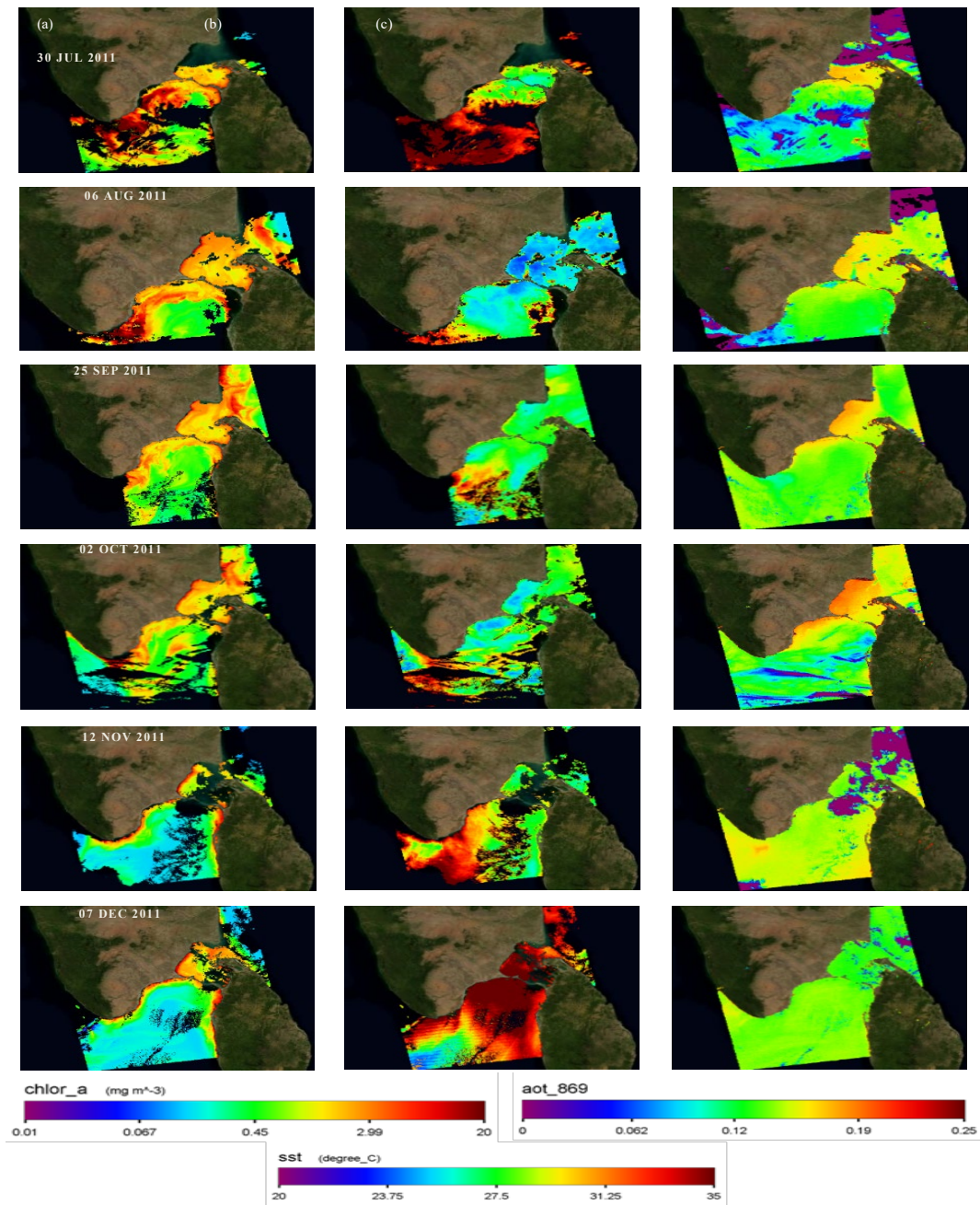


Fig.4. (a) *Chl-a* concentration trend over Gulf of Mannar by using MODIS satellite sensor for the duration of 6-month from July to December 2011, (b) Aerosol optical depth measurement during the study period and (c) Sea surface temperature measurement during the study period. Color bar scale represents the relative changes corresponding to the dimensional trend with respect to the *Chl-a* concentration, *AOT* and *SST* values.

The *Chl-a*, *AOT* and *SST* measurements are obtained from the global MODIS ocean color satellite. Data collection from satellite involves frequent measurements over time with large spatial coverage which is useful for assessing long-term changes. The *Chl-a* concentration in Gulf of Mannar shows different seasonal variability for different regions. The *Chl-a* concentration and *SST* is highly dependent due to the difference in gaining the heat between shallow and deeper portion of sea. The deeper sea observes high temperature. The surface water

in the middle region gains low temperature than the water in near shore. Increase in surface temperature in the shallow water increases the concentration of Chl-a, while an increase in surface temperature in the deeper water tends to decrease the concentration of Chl-a. During summer, in shallow regions closer to land, the water temperature may exceed even the atmospheric temperature. GOM is characterized by high salinity and surface temperature during the northeast monsoon. When more heat is absorbed in the ocean, surface temperature increases, and the ocean circulation patterns transport warm and cold water around the globe. From fig.3a very low numbers of chlorophyll concentration appears in light green and high chlorophyll concentrations appears in dark orange. The observations were taken from the MODIS sensor on NASA's Aqua satellite. The satellites measure the temperature of the top millimetre of the ocean surface. From fig.3c, the coolest waters temperature appears in blue and the warmest temperatures appears in red. In the Gulf of Mannar, the Northeast Monsoon is steadiest in January and is weak by the month of March. The wind becomes light and variable toward the end of April.

The northern part of GOM experiences high surface pigment concentration. The waters are very shallow compared to other surrounding waters of the island. Thus, the water contains other substance like suspended particles and dissolved organic matter in addition to *Chl-a*. From the above figure, *Chl-a* concentration is high during the month of January which is due to the decrease in the *AOT* and the *SST*. *SST* is high during April, thus the *Chl-a* concentration and the *AOT* measurements is reduced due to high surface temperature. During the month of March-May, the *Chl-a* concentration was reduced when compared with the month January, which may be due to surface heating during summer. From the month of February-May there was no variation in chlorophyll concentration. During the month of June, the *Chl-a* concentration is low which is due to the increase in the surface temperature. The highest spatially mean *Chl-a* concentration is observed in the month of January and the lowest is observed in the month of June.

Spatial and temporal analysis shows that *SST* and *Chl-a* concentration in this area is greatly influenced by the monsoon. *Chl-a* is an indicator for photosynthesis present in the ocean. *Chl-a* concentration is influenced by climatic factors such as surface temperature and winds. In GOM, *Chl-a* concentration is high during the Northwest monsoon compared to the Southwest monsoon. The *Chl-a* concentration is high along the coast due to the nutrient rich run-off from land via rivers. Also in near shore, *Chl-a* variability was high and decreases with distance towards offshore. *Chl-a* concentration is affected by rainfall and river discharge. During southwest monsoon, *SST* is low compared to the Northwest monsoon, while *Chl-a* in the Northwest monsoon is higher than Southwest monsoon. After the SW monsoon, the southwest coasts have higher surface pigment concentrations. In the SW monsoon the satellite data were not available, in which these waters are rich in *Chl-a* concentration. During Southwest monsoon period from the month of July to September high wind speed and decrease in surface temperature is observed around the south-eastern coast. Hence increase in chlorophyll concentration is observed from the month of August to October, 2011.

Fig. 4. represent the *Chl-a*, *AOT* and the *SST* measurements over the Gulf of Mannar by MODIS satellite sensor for the 6-month duration from July to December, 2011. Color bar scale represents the relative changes corresponding to the dimensional trend with respect to the *Chl-a* concentration, Aerosol depth measurement and the surface temperature values. During the

month of July, the surface temperature measurement was very low. So, the reduction in the Chl-a concentration and the aerosol optical depth measurement is observed during the month of July which is due to the decrease in the surface temperature level. Fig.4a indicate that, the *Chl-a* concentration is high during the month of August and September. In the month of August due to high Chl-a concentration the aerosol optical depth measurement is low and an average range of surface temperature measurement. High *Chl-a* concentration in the month of September shows average range of *AOT* and surface temperature measurements. Increased level of Chl-a concentration and the aerosol optical depth measurement observed during the month of December experience average surface temperature. During the month of August-October, the southwest monsoon period, it results in the high *Chl-a* concentration which shows low range of *AOT* and average surface temperature measurements. High Chl-a concentration in the open ocean waters is observed due to upwelling rather than other particles. From fig.4b very high level of optical depth measurement is obtained during the month of December. So, due to increased aerosol measurement, the Chl-a concentration increases with low surface temperature.

#### 4.2. Long term time series analysis

The time series distribution of *Chl-a* concentration, *AOD* and *SST* data are obtained from MODIS sensors for the daily data from 2002 to 2020. The time series distribution of the long-term changes in *Chl-a* concentration was unevenly distributed over the years in station-1. The Chl-a concentration was high over the station 1 which may be due to the upwelling in the coastal region. Over the study period of about 19 years, monthly Chl-a showing a range of 1.8 to 2.7 mg m<sup>-3</sup> during the cooler months of January and February and about 1.5 to 2 mg m<sup>-3</sup> during the warmer months of July and August, indicating higher Chl-a concentrations during the latter period. This is likely due to coastal waters being calmer during the summer than in winter. Throughout the years, during warmer months the Chl-a concentration is about 2 mg m<sup>-3</sup> ranging from 1.8 to 2.2 mg m<sup>-3</sup> and during the colder months the average Chl concentration of about 2.4 mg m<sup>-3</sup> ranging from 2 to 2.7 mg m<sup>-3</sup> was observed.

The time series distribution of *SST* increases during the warmer months and decreases during colder months which may be due to the change in climatic condition, as shown in figure 5c. The annual average *SST* were observed during the 2011 of about 28.3°C. The overall analysis shows that GOM experiences an average *SST* of about 27.5°C. *SST* shows minimum in the month of July and reached maximum in the month of April. The time series distribution shows that the *AOT* values increases in linear were observed during the beginning of every year and gradually decreases to minimum values at the end of the year. The average range of *AOT* is about 0.15. High nutrients are observed during summer in which the temperature recorded is also high. The Chl-a concentration value are observed as high during the winter season.

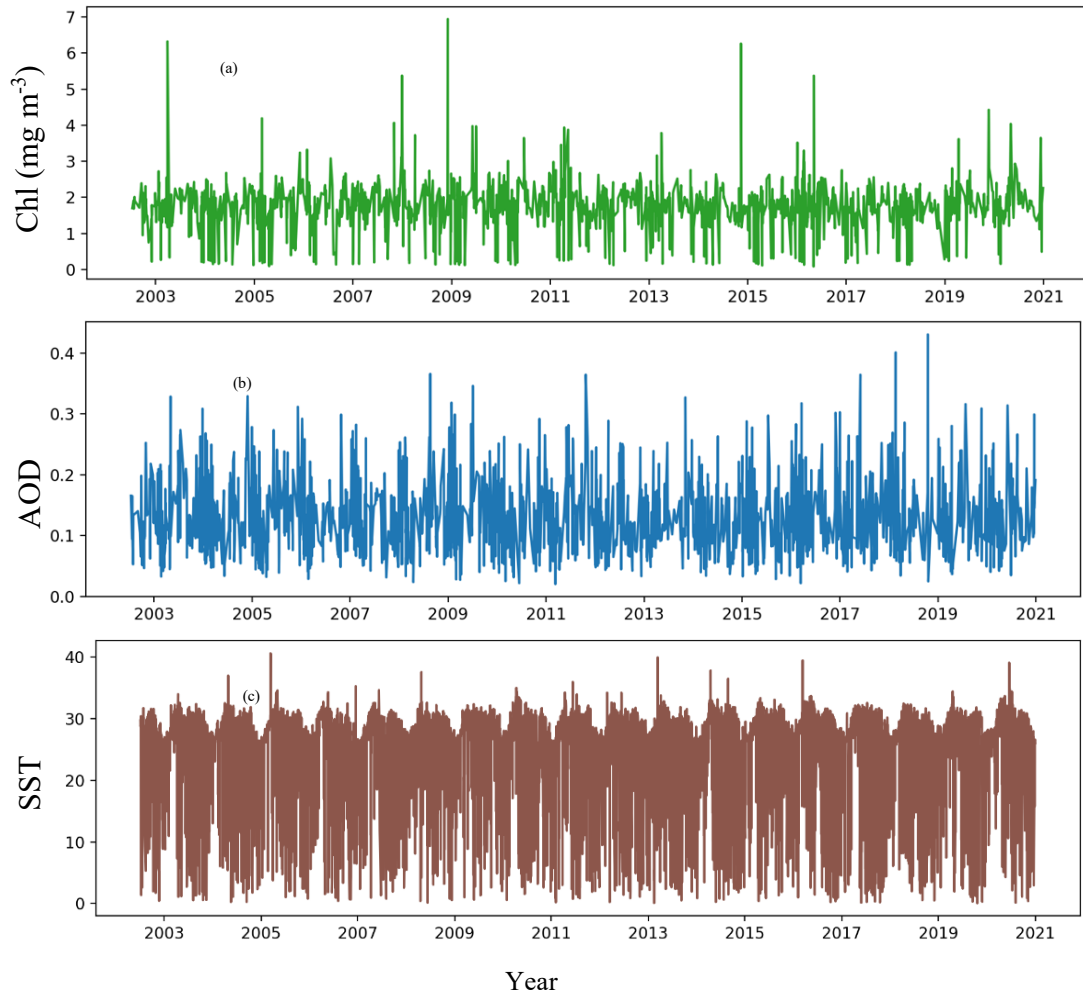


Fig. 5 Variation of Chl, AOD, and SST from MODIS data for location (st-1) over Gulf of Mannar from 2002 to 2020. (a) Time series representation of Chl data (b) time series representation of AOD data (c) Time series representation of SST data.

The time series distribution of *Chl-a* concentration, *AOD* and *SST* data for station 2 are obtained from MODIS sensors for the daily data from 2002 to 2020. The time series distribution of the long-term changes in *Chl-a* concentration, *AOD* and *SST* were unevenly distributed over the years in station-2. This station is located near the Pamban bridge, in which the moving of ship occurs which will affect the *Chl-a* concentration. The *Chl-a* concentration was low in this area which is due to several disturbance that occurs in the water. In the western season chlorophyll-a tends to be low, which is due to the strong tidal mixing causes the residence time of algae in the photic zone. Whereas in the east season chlorophyll-a will be higher. Monthly average *Chl-a* concentration ranges from 1.5 to 2.2 mg m<sup>-3</sup>. The distribution of *SST* in the east begins to rise in November to April with the increase in March, and decreased in May to October with the lowest *SST* in August. The monthly long-term variation for the *SST* from 2002 to 2020 shows that high surface temperature with an average of about 30°C. Due to high sea surface temperature the *Chl-a* concentration for this area gets reduced. The monthly variation data of *AOT* shows an average of about 0.15 to 0.18.

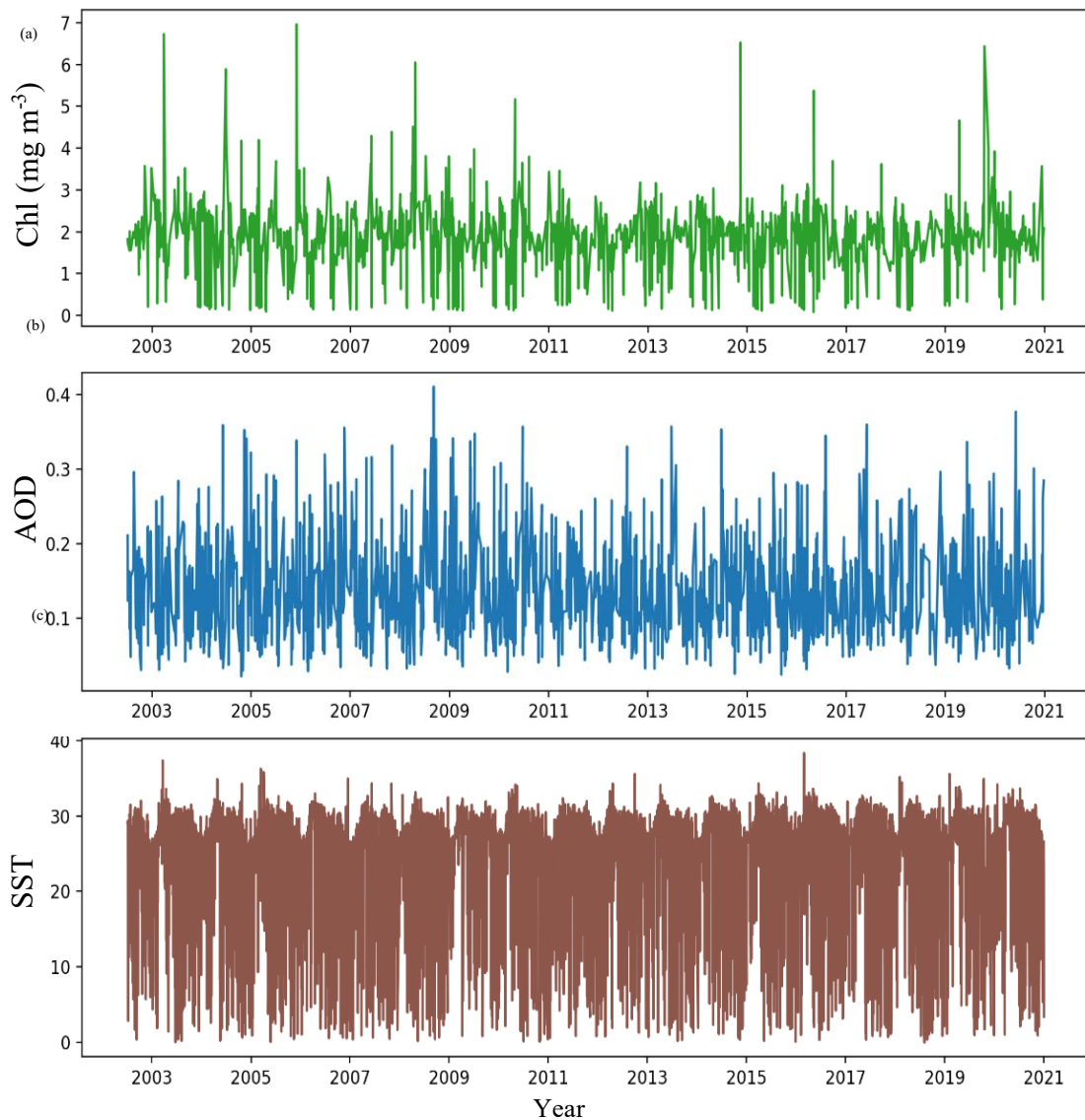


Fig. 6 Variation of Chl, AOD, and SST from MODIS data for location (st-2) over Gulf of Mannar from 2002 to 2020. (a) Time series representation of Chl data (b) time series representation of AOD data (c) Time series representation of SST data.

## 5. Conclusion:

Understanding the variations in Chl-a, SST, and AOD in the GoM is crucial, as these parameters significantly influence marine ecosystems and living organisms. The GoM's environmental conditions are particularly unique due to the presence of coral reefs, seagrass beds, and mangroves, which serve as essential habitats for various marine species by providing spawning, feeding grounds, and shelter. This study examines the variability of Chl-a in relation to environmental parameters using a satellite-based correction procedure for estimating Chl-a concentration, bypassing the need for additional validation steps with in-situ data, as previous research has established the accuracy of satellite-derived measurements. By analysing MODIS satellite data from 2011, we explored the spatio-temporal variability of Chl-a, AOD, and SST across the GoM. Our results indicate that Chl-a concentrations are generally lower in coastal

regions compared to open waters. Additionally, a time-series analysis of Chl-a from 2002 to 2020 revealed correlations between Chl-a, AOD, and SST, showing that increases in SST and AOD tend to coincide with decreases in Chl-a, and vice versa. Seasonal fluctuations in SST, AOD, and Chl-a concentrations further suggest that changes in seawater temperature and salinity play a significant role in regulating Chl-a levels.

The study also concludes that Chl-a concentration decreases with increasing water depth and distance from the shoreline, and that Chl-a exhibits a strong correlation with physical parameters such as SST and salinity. The findings of this study provide valuable insights for the remote sensing community, contributing to the understanding of marine ecosystems and supporting efforts to identify potential fishing zones. Future work should focus on expanding the spatial coverage of this research and incorporating in-situ or ground truth data to validate satellite observations in other regions where satellite data may be limited.

## 6. Acknowledgements:

The authors would like to express their gratitude towards Chennai Institute of Technology, Chennai, Tamil Nadu and Geosensing and Imaging Consultancy, Trivandrum for successfully carrying out this work.

## References:

1. Al-Tae, I. A. A. **2018**. "Salinity effect chlorophyll significantly". *Plant Archive*, 18(1), 723-726.
2. Bailey, S. W.; Franz, B. A.; and Werdell, P. J. **2010**. "Estimation of near-infrared water-leaving reflectance for satellite ocean color data processing". *Opt. Exp.* 18, 7521–7527.
3. Balasubramanian, S.; Shanmugam, P. **2015**. "Modelling of underwater light fields in turbid and eutrophic waters: Application and validation with experimental data". *Ocean Science*.
4. Banse, K.; Vijayaraghavan, S.; Madhupratap, M. **1996**. "On the possible causes of the seasonal phytoplankton blooms along the southeast coast of India". *Ind. J. Mar. Sci.*, 25, 283-289.
5. Barton, I. J. **1995**. "Satellite-derived Sea surface temperatures: current status". *J. Geophys. Res.*, 100, pp. 8777-8790
6. Brewin, R. J. W.; Sathyendranath, S.; Platt, T.; Bouman, H.; Ciavatta, S.; Dall'Olmo, G.; Dingle, J.; Groom, S.; Jönsson, B.; Kostadinov, T. S.; Kulk, G.; Laine, M.; Martínez-Vicente, V.; Psarra, S.; Raitos, D.E.; Richardson, K.; Rio, M.-H.; Rousseaux, C.S.; Salisbury, J.; Shutler, J.D.; Walker, P. **2021**. "Sensing the ocean biological carbon pump from space: a review of capabilities, concepts, research gaps and future developments". *Earth Sci. Rev.*, 217 (2021), Article 103604,
7. Brochier, T.; Echevin, V.; Tam, J.; Chaigneau, A.; Goubanova, K.; Bertrand, A. **2013**. "Climate change scenarios experiments predict a future reduction in small pelagic fish recruitment in the Humboldt Current system". *Global Change Biology*. 19(6):1841-53.
8. Cannizzaro, J. P.; Carder, K. L. **2006**. "Estimating chlorophyll-a concentrations from remote sensing reflectance in optically shallow waters", *Remote Sensing of Environment*, 101, 13-24.

9. Chen, J.; Zhang, X.; & Quan, W. **2013**. “Retrieval chlorophyll-a concentration from coastal waters: three-band semi-analytical algorithms comparison and development”. *Optics Express*, 21(7), 9024.
10. Dierssen, H.M. **2010**. “Perspectives on empirical approaches for ocean color remote sensing of chlorophyll in a changing climate”. *Proceedings of the National Academy of Sciences* 107, 17073–17078.
11. Giles, D. M.; Sinyuk, A.; Sorokin, M. G.; Schafer, J. S.; Smirnov, A.; Slutsker, I.; Eck, T. F.; Holben, B. N.; Lewis, J. R.; Campbell, J. R.; Welton, E. J.; Korkin, S. V.; Lyapustin, A. I. **2019**. “Advancements in the Aerosol Robotic Network (AERONET) Version 3 database – automated near-real-time quality control algorithm with improved cloud screening for Sun photometer aerosol optical depth (AOD) measurements”. *Atmos. Meas. Tech.*, 12, 169–209.
12. Gitelson, A.; Garbuzov, G.; Szilagyi, F.; Mittenzwey, K. H.; Karnieli, A.; Kaiser, A. **1993**. “Quantitative remote sensing methods for real-time monitoring of inland waters quality”. *Int. J. Remote Sens.*, 14, pp. 1269-1295,
13. Gordon, H. R and Wang, M. **1994**. “Retrieval of water-leaving radiance and aerosol optical thickness over the oceans with SeaWiFS: a preliminary algorithm,” *Appl. Opt.* 33(3), 443–452.
14. Gordon, H. R.; Brown, O. B.; Evans, R. H.; Brown, J. W.; Smith, R. C.; Baker, K. S.; Clark, D. K. **1988**. “A semi-analytic radiance model of ocean color,” *J. Geophys. Res.* 93(D9), 10909–10924.
15. Gunasinghe, D. S.; Weerasingha, D. B.; Ratnayake, A. S. **2024**. “Seasonal variations in chlorophyll-a and sea surface temperature in the exclusive economic zone of Sri Lanka”. *Remote sensing Applications: Society and Environment*, volume 34, 101197.
16. Gupta, S.; Baronia, A.; Lawrence, T. S.; Sankaradass, V.; Saravanan, V.; Jayanthiladevi, A. **2024**. “Development of OCDMA system in spectral/temporal/spatial domain for non-mapping/MS/MD codes”. *J Opt* **53**, 959–967.
17. Gurlin, D.; Gitelson, A.A.; Moses, W.J. **2011**. “Remote estimation of chl-a concentration in turbid productive waters—Return to a simple two-band NIR-red model?”. *Remote Sens. Environ.* 115, 3479–3490.
18. Hu, C.; Lee, Z.; Franz, B. **2012**. “Chlorophyll- a algorithms for oligotrophic oceans: A novel approach based on three-band reflectance difference”, *Journal of Geophysical Research* 117, C01011.
19. Huang, X. and Ding, A. **2021**. “Aerosol as a critical factor causing forecast biases of air temperature in global numerical weather prediction models”. *Sci. Bull.*, 18, 1917–1924.
20. Huot, Y.; Babin, M.; Bruyant, F.; Grob, C.; Twardowski, M. S.; Claustre, H.; Claustre, H. **2007**. “Does chlorophyll a provide the best index of phytoplankton biomass for primary productivity studies?”. *European Geosciences Union*.
21. IOCCG, **2006**. “Remote Sensing of Inherent Optical Properties: Fundamentals, Tests of Algorithms, and Applications, (ed. Z-P. Lee). International Ocean-Colour Coordinating Group (IOCCG), Reports of the International Ocean-Colour Coordinating Group, No. 5, Dartmouth, NS, Canada”.
22. Ishizaka, J. **2010**. “Climate Change and Marine Ecosystem, International Archives of The Photogrammetry, Remote Sensing and Spatial Information Science”, in *International Archives of the Photogrammetry, Remote Sensing and Spatial Information Science XXXVIII Part 8*, Kyoto, Japan.
23. Kilpatrick, K. A.; Podestá, G.; Walsh, S.; Williams, E.; Halliwell, V.; Szczodrak, M.; Brown, O.B.; Minnett, P.J.; Evans, R. **2015**. “A decade of sea surface temperature from MODIS”. *Remote Sens. Environ.*, 165 (2015), pp. 27-41.

24. Koponen, S.; Attila, J.; Pulliainen, J.; Kallio, K.; Pyhalahti, T.; Lindfors, A.; Rasmus, K.; Hallikainen, M. **2007**. “A case study of airborne and satellite remote sensing of a spring bloom event in the Gulf of Finland”. *Cont. Shelf Res.* 2007, 27, 228–244.
25. Le, C.; Hu, C.; Cannizzaro, J.; English, D.; Muller-Karger, F.; Lee, Z. **2013**. “Evaluation of chlorophyll-a remote sensing algorithms for an optically complex estuary”. *Remote Sens. Environ.* 2013, 129, 75–89.
26. Li, Y.; Xue, Y.; Guang, J. **2018**. “Ground-Level PM2.5 Concentration Estimation from Satellite Data in the Beijing Area Using a Specific Particle Swarm Extinction Mass Conversion Algorithm”. *Remote Sens.-Basel*, 10, 1906.
27. Mahpeykar, O and Khalilabadi, M. R. **2021**. “Numerical modelling the effect of wind on Water Level and Evaporation Rate in the Persian Gulf”. *International Journal of Coastal and Offshore Engineering*, 6(1), 47-53.
28. Matthews, M.W.; Bernard, S.; Robertson, L. **2012**. “An algorithm for detecting trophic status (chlorophyll-a), cyanobacterial-dominance, surface scums and floating vegetation in inland and coastal waters”. *Remote Sens. Environ.*, 124 (2012), pp. 637-652,
29. McMillin, L. M. **1975**. “Estimation of sea-surface temperatures from two infrared window measurements with different absorption”. *J. Geophys. Res.*, 80, pp. 5113-5117
30. Mobley, C. D. **1999**. “Estimation of the remote-sensing reflectance from above-surface measurements”. *Appl. Opt.*, 38, p. 7442,
31. Mondal, S and Lee, M.-A. **2024**. “Long-Term observations of sea surface temperature variability in the Gulf of Mannar”. *J. Mar. Sci. Eng.* 11(1), 102.
32. Morel, A., and Maritorena, S. **2001**. “Bio-optical properties of oceanic waters: A reappraisal”. *J. Geophys. Res.*, 106: 7163-7180.
33. Morel, A.; Prieur, L. **1977**. “Analysis of Variations in Ocean Color”. *Limnology and Oceanography*, 22, pp. 709-722
34. Nurdin, S.; Mustapha, M.A.; Lihan, T. **2013**. “The relationship between sea surface temperature and chlorophyll-a concentration in fisheries aggregation area in the archipelagic waters of Spermonde using satellite images”. In *AIP Conference Proceedings*; American Institute of Physics: New York, NY, USA.
35. O’Reilly, J. E., Werdell, P. J. **2019**. “Chlorophyll algorithms for ocean color sensors - OC4, OC5 & OC6”. *Remote Sensing of Environment*, 229, 32–47.
36. O’Reilly, J. E.; Maritorena, S.; Mitchell, B. G.; Siegel, D. A.; Carder, K. L.; Garver, S.A.; Kahru, M.; McClain, C. **1998**. “Ocean color chlorophyll algorithms for SeaWiFS”. *J. Geophys. Res.*, 103 (1998), pp. 24937-24953,
37. Pahlevan, N.; Mangin, A.; Balasubramanian, S.V.; Smith, B.; Alikas, K.; Arai, K.; Barbosa, C.; Belanger, S.; Binding, C.; Bresciani, M.; Giardino, C.; Gurlin, D.; Fan, Y.; Harmel, T.; Hunter, P.; Ishikaza, J.; Kratzer, S.; Lehmann, M.K.; Ligi, M.; Ma, R.; Lauzer, F.-R.M.; Olmanson, L.; Opeeltt, N.; Pan, Y.; Peters, S.; Reynaud, N.; Carvalho, L.A.S.; Simis, S.; Spyarakos, E.; Steinmetz, F.; Stelzer, K.; Sterckx, S.; Tormos, T.; Tyler, A.; Vanhellefont, Q.; Warren, M. **2021**. “ACIX-Aqua: A global assessment of atmospheric correction methods for Landsat-8 and Sentinel-2 over lakes, rivers, and coastal waters”. *Remote sensing of environment*, 258.
38. Pahlevan, N.; Smith, B.; Schalles, J.; Binding, C.; Cao, Z.; Ma, R.; Alikas, K.; Kangro, K.; Gurlin, D.; Hà, N.; et al. **2020**. “Seamless retrievals of chlorophyll-a from Sentinel-2 (MSI) and Sentinel-3 (OLCI) in inland and coastal waters: A machine-learning approach”. *Remote Sens. Environ.* 2020, 240, 111604.
39. Patissier, D.-B.; Gower, J.F.R.; Dekker, A.G.; Phinn, S.R.; Brando, V.E. **2014**. “A review of ocean color remote sensing methods and statistical techniques for the detection, mapping and analysis of phytoplankton blooms in coastal and open oceans”. *Prog. Oceanogr.* 2014, 123, 123–144.

40. Paytan, A.; Mackey, K. R.; Chen, Y.; Lima, I. D.; Doney, S. C.; Mahowald, N.; Labiosa, R.; Post, A. F. **2009**. "Toxicity of atmospheric aerosols on marine phytoplankton". *Proceedings of the National Academy of Sciences*, 106(12), pp.4601-4605.
41. Platt, T.; & Sathyendranath, S. **2008**. "Ecological indicators for the pelagic zone of the ocean from remote sensing". *Remote Sensing of Environment*, 112(8), 3426–3436.
42. Schalles, J. F. **2006**. "Optical remote sensing techniques to estimate phytoplankton chlorophyll a concentrations in coastal waters with varying suspended matter and cdm concentrations". *Remote Sensing and Digital Image Processing, Remote Sensing and Digital Image Processing*, Springer International Publishing, pp. 27-79
43. Shen, M.; Duan, H.; Cao, Z.; Xue, K.; Qi, T.; Ma, J.; Liu, D.; Song, K.; Huang, C.; Song, X.; et al. **2020**. "Sentinel-3 OLCI observations of water clarity in large lakes in eastern China: Implications for SDG 6.3. 2 evaluation. *Remote Sens. Environ.* 2020, 247, 111950.
44. Simon, A.; and Shanmugam, P. **2012**. "An Algorithm for Classification of Algal Blooms Using MODIS-Aqua Data in Oceanic Waters around India," *Advances in Remote Sensing*, 1, 35- 51.
45. Tholkapiyan, M. **2012**. "Derivation of Calibration Coefficients for OCM-2 Sensor for Coastal Waters". *Journal of Geophysics & Remote Sensing*, 01(02).
46. Tian, B.; Wu, W.; Yang, Z.; Zhou, Y. **2016**. "Drivers, trends, and potential impacts of long-term coastal reclamation in China from 1985 to 2010". *Estuar. Coast. Shelf Sci.* Volume 170, 83-90.
47. Tong, Y.; Feng, L.; Zhao, D.; Xu, W.; Zheng, C. **2022**. "Remote sensing of chl-a concentrations in coastal oceans of the Greater Bay Area in China: Algorithm development and long-term changes". *Int. J. Appl. Earth Obs. Geoinf.* 112, 102922.
48. Vanhellemont, Q and Ruddick, K. **2018**. "Atmospheric correction of metre-scale optical satellite data for inland and coastal water applications". *Remote Sensing of Environment* 216, 586–597.
49. Vanhellemont, Q. **2019**. "Adaptation of the dark spectrum fitting atmospheric correction for aquatic applications of the Landsat and Sentinel-2 archives". *Remote Sensing of Environment* 225, 175–192.
50. Werdell, P. J.; McKinna, L. I. W.; Boss, E.; Ackleson, S. G.; Craig, S. E.; Gregg, W. W.; Lee, Z.; Maritorena, S.; Roesler, C. S.; Rousseaux, C. S.; Stramski, D.; Sullivan, J. M.; Twardowski, M. S.; Tzortziou, M.; Zhang, X. **2018**. "An overview of approaches and challenges for retrieving marine inherent optical properties from ocean color remote sensing". *Prog. Oceanogr.*, 160, pp. 186-212,